

Document downloaded from:

<http://hdl.handle.net/10251/138901>

This paper must be cited as:

Martorell-Tejedor, S.; Tortajada-Genaro, LA.; Maquieira Catala, A. (27-1). Magnetic concentration of allele-specific products from recombinase polymerase amplification. *Analytica Chimica Acta*. 1092:49-56. <https://doi.org/10.1016/j.aca.2019.10.006>



The final publication is available at

<https://doi.org/10.1016/j.aca.2019.10.006>

Copyright Elsevier

Additional Information

Magnetic concentration of allele-specific products from recombinase polymerase amplification

Sara Martorell,^{a,b} Luis A. Tortajada-Genaro,^{*,a,b,c} and Ángel Maquieira^{*,a,b,c}

^a Instituto Interuniversitario de Investigación de Reconocimiento Molecular y Desarrollo Tecnológico (IDM), Universitat Politècnica de València-Universitat de València, Camino de Vera s/n, E46022 Valencia, Spain.
E-mail: luitorge@qim.upv.es, amaqueira@qim.upv.es

^b Unidad Mixta UPV-La Fe, Nanomedicine and Sensors, IIS La Fe, Valencia, Spain

^c Departamento de Química, Universitat Politècnica de València Valencia, Spain

Abstract

The studied challenge is the specific detection of low-abundant genomic variants that differ by a single nucleotide from the wild type. The combination of blocked recombinase polymerase amplification (RPA) and selective capture by probes immobilised on magnetic-core particles integrated into a flow system is presented. The sensing principle was demonstrated as the effective concentration-detection of the specific generated products was achieved. The analytical performance of resulting assay was successfully compared to PCR-based methods or array formats, providing faster effective detection of the selective products. As proof of concept, the single-nucleotide substitutions of the *KRAS* gene at codon 12 were studied in chip with parallel microchambers and permanent magnets. The blocked RPA products (generated at 37 °C) from tumour biopsies (extracted DNA 4 ng) provided a specific fluorescent bead-line that depends on the present mutation. The results agree with those reported by next-generation sequencing and provide new opportunities for *in vitro* diagnostic and personalised medicine.

Keywords: isothermal amplification; magnetic beads; in-chip hybridization; DNA genotyping; optical biosensing

30 **1. Introduction**

31 Molecular technologies has advanced the identification of the genomic diversity and their
32 role in human diseases [1]. Implementing a personalised approach into patient care
33 needs fast-response methods that are cost-effective and compatible with low-resource
34 settings to solve the limitations of technically skilled personnel and specialized
35 infrastructures. Early diagnostics reduces disease effects and health-care expenses. A
36 conventional methodology relies on the selective recognition of the sequence-specific
37 oligonucleotides on active electrodes or passive planar chip surfaces, and subsequent
38 signal transduction in integrated microsystems [2]. Another successful approach is
39 based on oligonucleotide-coated particles, which involves fewer technical requirements,
40 a bigger surface area, easy chemical modification and effective mixing with samples
41 [3,4]. Micro-sized magnetic beads have been the most extensively applied in diagnostic
42 chips as the external magnetic field (electro-magnets, coils or permanent magnets)
43 controls their movement [4,5]. The selective magnet-induced isolation of the molecules
44 captured to particles improves the assay selectivity and sensitivity [6]. Furthermore,
45 these assays reduce both volumes of reagents and samples and cuts the time required
46 for target molecules to diffuse to the interrogating probes [7]. Their use has enabled well-
47 established protocols for the simplified extraction, amplification and detection of nucleic
48 acids. Thus the microfluidic systems yield a platform that facilitates the rapid and
49 automated DNA analyses [8,9].

50 One common limitation of these methods is that the need for a DNA amplification step
51 to achieve a copy number big enough to be detected. The consequences are complex
52 platforms for DNA-based diagnostic tools with a high demand for the auxiliary
53 instrumentation. To overcome some of these drawbacks, several isothermal techniques
54 have been developed, and their integration into microsystems or portable devices has
55 improved nucleic acid-based on-site assays [10]. Probe-conjugated magnetic beads
56 have recognised specific templates from clinical sample lysates and are later amplified
57 by either loop-mediated isothermal amplification (LAMP) [11] or rolling circle
58 amplification (RCA) [12]. Regarding to detection, promising assays combine a linear
59 RCA-type amplification and later particle aggregation [13]. However, other enzymatic
60 methods can potentially perform better (e.g. high yield, exponential reaction kinetics,
61 lower temperature). Recombinase polymerase amplification (RPA) is an unexplored
62 candidate, despite being one of most sensitive and selective isothermal techniques, with
63 excellent operational conditions for integrated devices [14].

64 We herein firstly report research that focused on the selective capture of RPA products
65 onto probe-conjugated microbeads confined within a microfluidic channel and using a
66 permanent magnet. This challenge spans from the impact on the hybridisation kinetics
67 and to the assay integration, and includes the dynamics during magnetic-concentration.
68 Due to the amplification mechanism, the nature of the RPA mixture is complex and an
69 influence on the detection of the generated products compared to PCR or other
70 isothermal techniques was expected, as reported previously [15].

71 The aim of the presented approach is the concentration of allele-specific products from
72 RPA using magnetic beads for the sensitive identification of single-point mutations. The
73 detection of these variations in the genome is important because they have been
74 associated with disease progression and treatment efficiency [16]. Although some
75 examples describe the discrimination of single-nucleotide mismatches based on allele-
76 specific hybridisation to probes anchored on magnetic beads [8,17,18], they all are
77 restricted by the PCR amplification technique. For achieving the challenge of specific
78 discrimination, an affordable fast-response method was developed, based on blocked
79 isothermal amplification, bead-based hybridization, magnetic concentration and optical
80 detection. Our empirical goal was to establish the principles and experimental conditions
81 for the differential capture and detection of the RPA products in a microfluidic system. In
82 case of a correct discrimination of single-base variants, patients could be classified in
83 the adequate group and the suitable treatment could be applied as personalised
84 medicine.

85

86 **2. Experimental**

87 2.1 Chip assembly

88 The micro-system was composed of a supporting platform and microfluidic chips that
89 enable the simultaneous analysis of eight samples. The 3D-printed platform, designed
90 using the CAD-3D Autodesk inventor (Autodesk, USA), was manufactured in polylactic
91 acid (PLA, RS Components, UK). The printing technology was fused filament fabrication
92 (The Ultimaker Cura 2, Ultimaker, Netherlands). The printing parameters were: nozzle
93 0.4 mm; layer height 0.1 mm; infill density 100%; print speed 60 mm/s; travel speed 120
94 mm/s; print temperature 210 °C and bed temperature 60 °C. Eight neodymium magnets
95 (dimensions 2.2×0.5×5 mm, vertical force 0.1 kg, slip resistance 0.02 kg) were
96 integrated. The microfluidic chip, manufactured in cyclic olefin polymer, contained eight
97 20 µL-rhombic chamber reactors (ChipShop, Germany). The dimensions of each

98 chamber were 4 mm×13.8 mm×0.35 mm. The chip was aligned to the platform by placing
99 the magnets below the middle of the chip.

100

101 2.2 Target

102 As proof of concept, the method was developed to analyse hotspots in the *KRAS* gene.
103 Single-base substitutions of this oncogene are extensively investigated as genetic
104 markers in human cancer pathogenesis and therapies [19]. We specifically identified the
105 most frequent mutations (codon 12), which were p.G12C (c.34G>T, rs121913530),
106 p.G12S (c.34G>A, rs121913530) and p.G12V (c.35G>T, rs121913529). Primer and
107 probes were designed by considering the thermodynamic parameters of recognition
108 process. Bioinformatic tools (OligoCalc software, Northwestern University, USA)
109 reported that the selected sequences were unlikely to form internal hairpin structures,
110 self-dimers or heterodimers. The used oligonucleotides were supplied by Eurofins
111 (Germany).

112

113 2.3 Conjugation of particles

114 A set of magnetic-core particles coated with probes (wild-type and mutants p.G12C,
115 p.G12S and p.G12V) were prepared. The selected particles were Dynabeads MyOne
116 carboxylic acid (Invitrogen, NY, USA). Beads (7.12×10^8) were washed with 2-(N-
117 morpholino)-ethanesulfonic acid buffer (MES, 100 mM, pH 4.8) (Sigma-Aldrich) for 30
118 min (2 times) and resuspended. A total of 0.6 nmol amino-modified probe (NH₂-C₆-T₅-
119 AGTTGGAGCTNGTGGCGTAGG, N = A, C, T or G) in MES buffer with ethyl
120 carbodiimide hydrochloride (1.25 M) was added and incubated (overnight, room
121 temperature). Then beads were washed 3 times with Tris-Tween buffer (1 M of Tris 1 M,
122 10 % of Tween 20, pH 8) and suspended in Tris-EDTA buffer (1 M of Tris, 100 mM of
123 EDTA, pH 8). Functionalisation efficiency was quantified by determining the probe
124 excess in relation to its initial concentration (absorbance at $\lambda=260$ nm).

125

126 2.4 DNA extraction and amplification

127 For the optimisation assays, two cell cultures were used, cell line SK-N-AS (ATCC, wild-
128 type for *KRAS* codon 12) and cell line HCT 116 (ATCC, c.38G>A), from a primary
129 carcinoma tissue. For method validation, healthy and oncological patients were recruited

130 for the present study according to ethics regulations. QIAcube robotic workstation
131 (Qiagen, Germany) extracted genomic DNA from 5- μ m thick formalin-fixed paraffin-
132 embedded tissue sections. The used reagents were mini kit FFPE Qiagen. The
133 concentration of the DNA extracts ($\text{ng } \mu\text{L}^{-1}$) was obtained by spectrophotometry using
134 NanoDrop 2000c (ThermoFisher Sci., USA), and by fluorimetry using Qubit dsDNA HS
135 Assay Kit (ThermoFisher Sci.).

136 The reagents used for the genomic DNA amplification came in the TwistAmp Basic RPA
137 kit (TwistDx, UK). The mixtures (50 μ L) for the blocked isothermal amplification were
138 prepared with the enzyme pellet in rehydrated buffer, 480 nM of magnesium acetate,
139 480 nM of upstream primer and downstream primer, 70 nM of blocking agent, 4 ng of
140 genomic DNA, 0.01 mM aminoallyl-dUTP-Cy5. The employed heating system was an
141 Eppendorf Thermomixer with MTP adapter (300 rpm, Eppendorf), operating at 37 °C for
142 40 min. Also, real time thermocycler (TS2, Qiagen) was used for the optimisation assay.
143 The reaction mechanism is described in Fig. SI.1.

144

145 2.5 In-chip assay

146 The amplification products (2 μ L) were mixed with 18 μ L of hybridisation buffer (1x saline
147 sodium citrate buffer, 30% formamide), containing beads conjugated with each specific
148 probe (final concentration 7.12×10^5 beads μL^{-1}). Solutions were loaded to chip by a
149 pressure-driven flow (20 μ L, < 3 s) (Fig. SI.2). Incubations were run at 95 °C for 10 min
150 (denaturation) and at 37 °C for 30 min (hybridisation). Then, the magnets retained the
151 magnetic particles inside each reaction chamber to enable the total removal of the
152 supernatant. The reactor was washed with 20 μ L of 0.01% SSC buffer (SSC 1 \times : 150 mM
153 sodium chloride-15 mM trisodium citrate pH 7.3).

154 A surface fluorescence reader imaged the bead-line in each reactor. This detector was
155 equipped with a high sensitivity charge coupled device camera (Retiga EXi, Qimaging
156 Inc., Canada), with light emitting diodes (Toshiba TLOH157P, Japan) and filters (λ_{ex} 635
157 nm, λ_{em} 670 nm). Intensities were also compared to those obtained by fluorescence
158 microscopy (Leica DCF 3000G, Germany). Image processing (segmentation and quality
159 assurance) was performed by reporting the bead-line and background intensities (mean
160 and standard deviation).

161 A discrimination factor was calculated to assign each patient to a genetic population
162 (wild-type, p.G12C, p.G12S or p.G12V). Specifically, the factor for a given population

163 was the relative response of the corresponding probe-conjugated bead in relation to all
164 the beads. The patient was assigned to the group with the highest discrimination factor.

165

166 2.6 Reference methods

167 Hybridisation on chip (colorimetric chip detection). The RPA products were detected and
168 identified by a hybridisation assay on rectangular slides (25 mm×75 mm). The protocol
169 is described in a previous paper [20]. Briefly, amine-DNA probes were immobilised on a
170 modified plastic chip. The format was four arrays per chip and four replicates per target.

171 The amplified products (5 µL) were mixed with 45 µL of hybridisation buffer, heated (95
172 °C, 5 min) and dispensed onto sensing arrays. After incubation (37 °C, 60 min), the
173 arrays were rinsed with progressive dilutions of hybridisation washing buffer. After
174 performing the colorimetric staining chip, the results were read.

175

176 *Sequencing.* Somatic mutations detection was performed by the Ion Torrent PGM
177 technology (ThermoFisher Scientific). The Oncomine Solid Tumor DNA kit enabled the
178 simultaneously analysis of hotspots mutations in 22 genes (included *KRAS* gene). A
179 multiplex PCR amplification of 10 ng of genomic DNA generated the DNA barcoded
180 libraries. The data from the sequencing runs were aligned to the hg19 human reference
181 genome and variant calling.

182

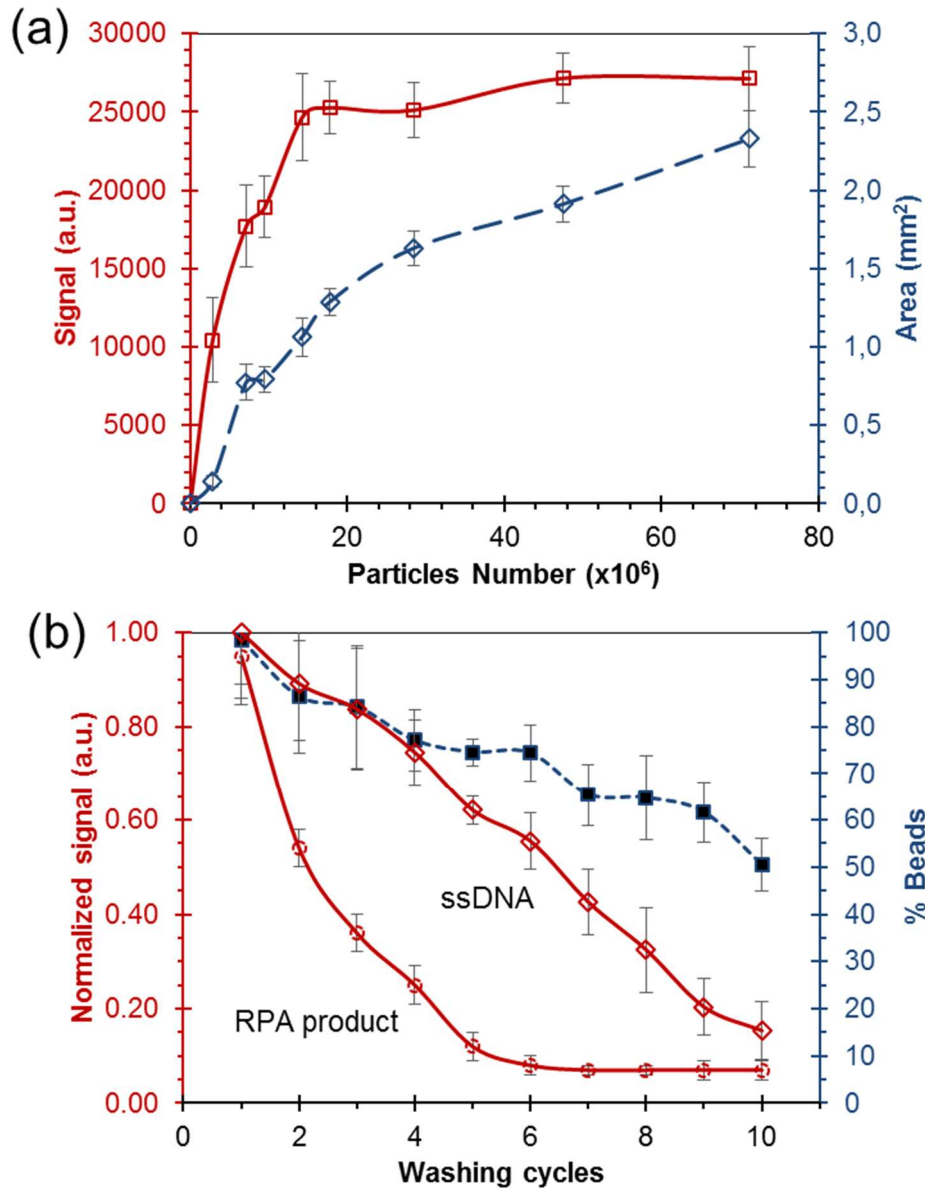
183 3. RESULTS AND DISCUSSION

184 3.1 Bead capture and concentration of RPA products

185 After an isothermal DNA amplification, the specific isolation of the products was studied,
186 based on the selective hybridisation onto beads and their magnetic concentration. A
187 relevant variable was the probe amount immobilised onto the magnetic-core particles.
188 Conjugation was performed to obtain optimal surface-probe density to maximise
189 hybridisation efficiency (probe density about 10^{12} molecules cm^{-2}). The selected
190 relationship between the 5'-amino-labelled probes and the carboxylic-functionalized
191 particles (1 µm diameter) was 8.4×10^{-19} moles per particle. Thus, an important of probe
192 excess was needed compared to the particle surface area (3.14×10^{-8} cm^2).

193 The number of probe-conjugated particles and the washing protocol are relevant
194 parameters for the hybridisation of DNA to the bead-immobilised probes confined within

195 a microfluidic channel [6,7,9]. Specific experiments were performed to establish the best
196 assay conditions. Fig. 1 shows that by increasing the bead number, the signal and the
197 area occupied by the magnetic particles in the reaction chamber were, respectively, more
198 intensive and bigger until saturation. The selected amount was 14.2×10^6 of probe-
199 conjugated beads for a rhombic chamber chip of 20 μL . A stringent hybridisation buffer
200 (low ionic strength buffer, high formamide content) favoured the perfect-match bonds
201 and reduced non-specific interactions. By increasing the number of wash cycles, the
202 percentage of the captured beads was lower. Also, the linear decreases in the bead-line
203 signal were observed for both single-strand DNA and RPA product, being higher for the
204 double-strand DNA. The results revealed a loss of particles despite of magnet action and
205 a major denaturation for the amplification products, respectively. Thus the method
206 succeeded in controlling the hybridisation and washing conditions, and yielded a final
207 concentration factor that ranged between 1:8 and 1:10.



208

209 *Fig. 1 (a) Effect of the number of particles on the hybridisation reaction. (b) Effect of wash*
 210 *cycle on the hybridisation reaction. Replicates = 3.*

211

212 Under those experimental conditions, the hybrids RPA product/probe were formed at low
 213 temperature (37 °C, about 20°C lower than the melting temperatures) for a short period
 214 (30 min). After applying the magnetic field and washing, the particle aggregation was
 215 induced and a packed bead-line was observed with a width of about 0.8 mm (Fig. SI.3).
 216 Null and low responses, comparable to those obtained for an empty microchamber, were
 217 observed for the probe-free particles and the non-complementary probe-conjugated
 218 particles, respectively. Thus, the method was reliable because significant fluorescent

219 responses were recorded only in the microchambers with the particles conjugated with
220 the complementary probes. Replicate experiments also confirmed that the method was
221 reproducible, obtaining a relative standard deviation of 15-20 %. Regarding the
222 sensitivity, the estimated detection limit was 250 copies of genomic DNA from biopsy
223 tissue.

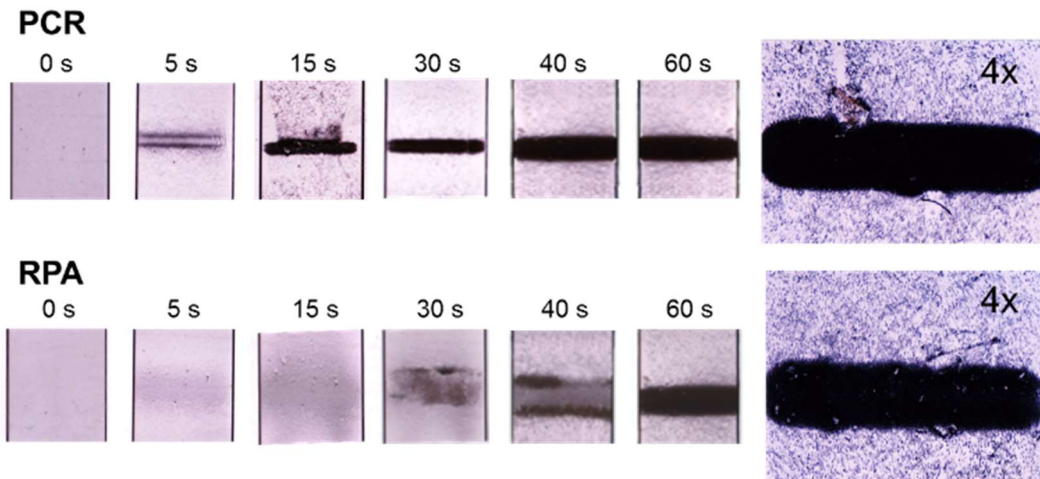
224

225 **3.2 Comparison with PCR-based method**

226 The proposed assay demonstrated a relevant potential for detecting DNA templates and
227 for being integrated onto point-of-care genetic platforms. The following experiments were
228 focused on the performances of the isothermal and the PCR-based approach [5,7,9].
229 The results showed that the capture yields (>90 %) were similar between RPA products
230 and PCR products, but the magnetic-induced concentration differed depending on the
231 employed amplification technique (Fig. 2). The movement of beads with PCR products
232 to the magnet zone was effective at 15 s, while the beads with RPA products needed 60
233 s and external flushing. This behaviour was related to the differences of reaction
234 composition of both enzymatic DNA amplifications. The RPA formulation contained a
235 high-molecular-weight polyethylene glycol (PEG) and crowing agents, used to facilitate
236 isothermal amplification and to reduce the mixing effects of thermal convection during
237 the reaction run at low temperatures [14]. However, these components negatively
238 affected the bead-based assay. In high-viscosity fluids like RPA media, the balance
239 between the drag (viscous resistance) and magnetic force led to a lower particle
240 velocities. Some groups of beads were aggregated through the microfluidic channel,
241 slowing down the bead-concentration towards the magnet. Nevertheless, the magnetic-
242 field-induced concentration of the RPA products was robust and effective in terms of the
243 final amount of beads over the magnet.

244 Other analytical performances, such as reproducibility, sensitivity and hybridization
245 selectivity were also similar. As expected, the main advantages of RPA derived from
246 their isothermal nature, such faster response (i.e. amplification 30 min RPA vs. 90 min
247 PCR) and minimal auxiliary instruments (i.e. unnecessary thermal cycler).

248



249

250 *Fig. 2 Sequential micrography of the magnetic-field-induced bead concentration into the*
 251 *microfluidic chip, depending on the used amplification technique. Magnification factor:*
 252 *10×. Target: wild-type variants of KRAS gene.*

253

254 **3.3 Comparison with the planar chip format**

255 The performances of homogeneous hybridisation on the magnetic particles in the
 256 microfluidic chamber chip was also compared against a conventional approach based
 257 on a heterogeneous format (array in chip) [2,20].

258 The hybridisation kinetics of RPA products at 37 °C were examined (Fig. 3a). A
 259 saturation-type curve was obtained at the 30-minutes incubation time for the assay
 260 based on magnetic beads in the microfluidic device, with 60 min for planar chip assays.
 261 The observed behaviours matched to the Langmuir model for DNA hybridisation [21],
 262 described by the following equation:

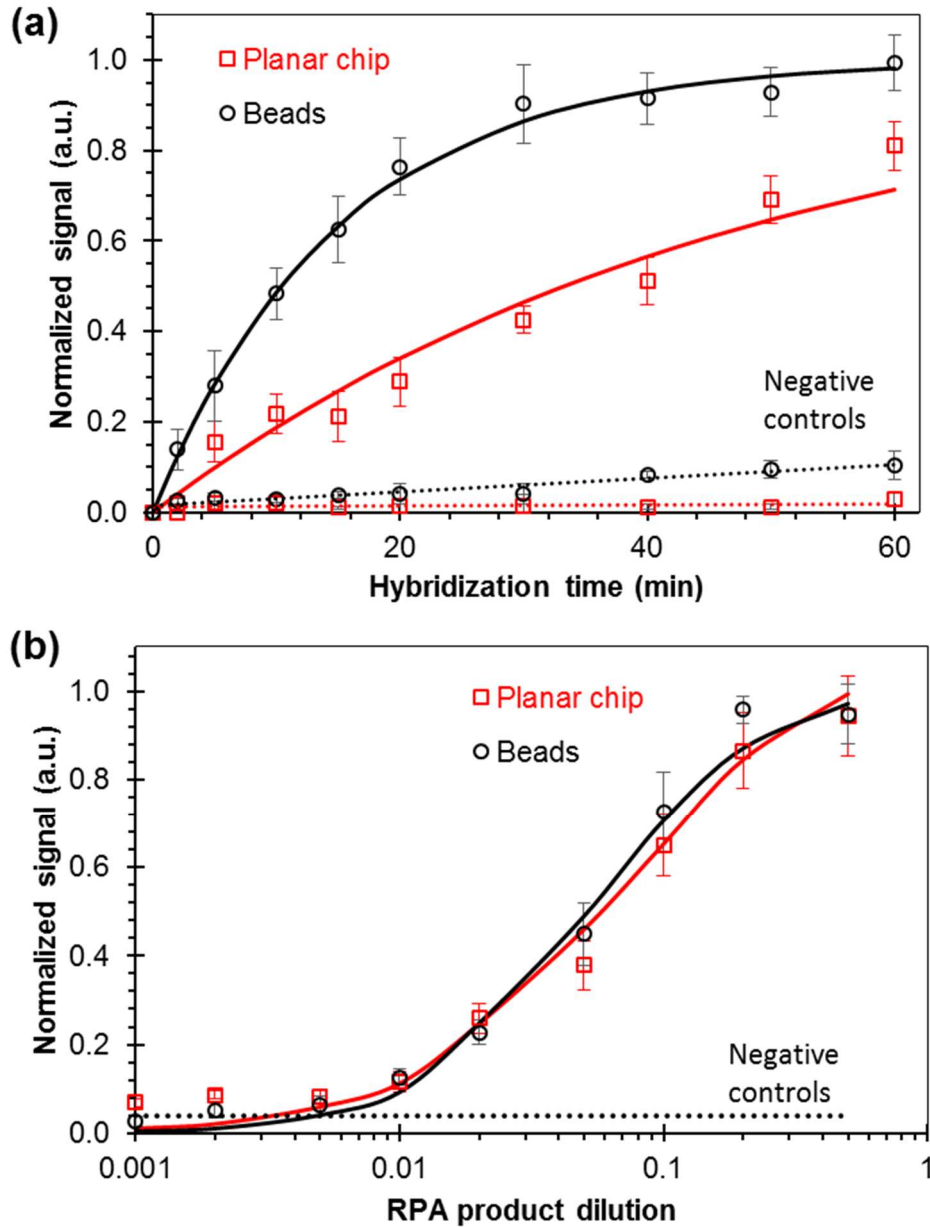
263
$$x(t) = x_{eq} \left[1 - \exp\left(-\frac{t}{\tau}\right) \right]$$

264 where $x(t)$ is the time dependent hybridisation fraction, x_{eq} the equilibrium hybridisation
 265 fraction and τ is related to the hybridisation rate constant (including the denaturation
 266 correction).

267 The estimated half-life times (τ -values) were 48.2 min for the planar chip format and 14.8
 268 min for the bead-based format with regression coefficients of 0.960 and 0.997,
 269 respectively. Thus, the hybridisation process of the RPA amplification products was
 270 faster with the probes immobilised on beads than on chip. The cause of these differences
 271 were examined. The estimated immobilization densities of specific probes were similar,

272 being 1-5 pmol cm⁻² for magnetic beads and 2-6 pmol cm⁻² for plastic chip. Also, the
273 number of binding sites, calculated from the active areas in both approaches, was
274 comparable. However, there are important differences in the reaction nature. In a planar
275 chip, the transportation process of target molecule for the bulky solution to the surface
276 must be considered, delaying the time required until the saturation. A homogeneous
277 format (i.e. solid-liquid interface) would need much longer time compared to the
278 heterogeneous format (i.e. liquid) [22].

279 For DNA-based diagnostic or prognostic, tests need to display high sensitivity because
280 numerous applications involve the detection of the target sequence present in small copy
281 numbers. To explore this detection capability, dilution experiments were performed,
282 using the amplification products obtained from genomic DNA. Fig. 3b shows that the data
283 fitted to a logistic response curve (regression coefficients 0.990-0.993). The limits of
284 detection, defined as the target amount and statistically differed from the negative
285 controls, were a dilution factor of RPA products about 1:200. These results agreed with
286 the lower hybridisation yields expected for the amplification products by considering the
287 competitiveness between the probe and the complementary strand for the same target
288 strand [5,7,15]. Assay reproducibility, obtained from replicate experiments and
289 expressed as relative standard deviation, ranged between 5% and 15%. The calibration
290 curves were similar for the homogeneous and heterogeneous formats (equation
291 parameters, t-test p-value >0.05, F-test p-value >0.05), which confirmed the feasibility of
292 the developed analytical approach.



293

294 Fig. 3 Comparison of planar chip and bead formats. a) Effect of hybridisation time on
 295 fluorescence signal. Fitting curve: $y = a \cdot (1 - e^{-x/b})$. b) Influence of the number of copies on
 296 fluorescence intensity. Incubation time: 60 min for the planar chip and 30 min for beads.
 297 Fitting curve: $y = L / (1 + a \cdot e^{-b \cdot x})$.

298

299 3.4 Enrichment of mutant variants

300 As proof of concept, the RPA-particle concentration method was applied in the
 301 challenging field of the detection of sequence changes. In case of single nucleotide
 302 variations, a high-selective amplification approach prior to the detection was required

303 because the mutant variants must be identified in a wild-type genomic DNA background.
304 A novel method for the preferential amplification of minority mutations before the
305 magnetic-based concentration was studied, called blocked RPA [20]. The hypothesis
306 was that the enrichment of these variants against the wild-type strand could induced,
307 based on the addition of a blocking oligonucleotide to the RPA reaction solution,
308 improving the latter on-bead hybridization.

309 The first stage was to select a wild-type blocker following a design criteria based on an
310 RPA mechanism and from the calculated thermodynamic properties. In order to reduce
311 the amplification in the primer annealing step, one restriction was for the blocker
312 candidates to partially overlap the upstream primer (clamp effect). This design avoids
313 the strand-displacing activity of the polymerase used in RPA (Bsu polymerase) if the
314 primer was bond to the template.

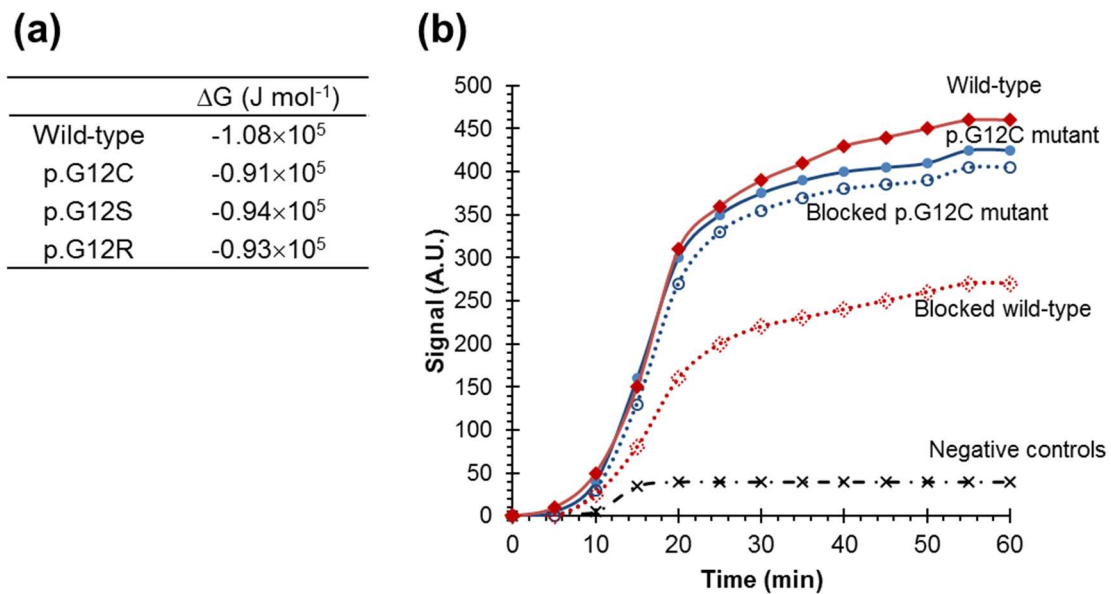
315 Moreover, the position of the hotspot in the blocking agent sequence drastically varied
316 the estimated stability of the mismatched hybrids. A central position allowed a variation
317 in free energy to lower between 1.5 and 1.7×10^5 J mol⁻¹ for the single-nucleotide
318 mutations (Fig. 4). According to these values, the blocker would compete with the
319 upstream primer for the same site in the wild-type strand. The DNA extracts from
320 control/mutant cell lines were amplified in the presence of the blocker (0-400 nm) by the
321 PCR and RPA approaches in solution format. If the blocking agent was absent, there
322 were no differences between the yield amplification of the wild-type and the mutant
323 templates (10^7 - 10^8 , test t: p=1.0). By increasing the concentration, the end-point
324 responses decreased in both mixtures. The experimental data were fitted to a four-
325 parameter logistic equation:

326
$$Signal = d + \frac{a - d}{1 + \left(\frac{[bloq]}{c}\right)^b}$$

327 where [bloq] is the blocking agent concentration, d is the background signal, a is the
328 signal for the lack of the blocking oligonucleotide, c is related to the concentration at the
329 inflection point and b is related to curve steepness. The c-parameter was related to the
330 effective blocking concentration that reduced the signal to half. The values were 46 ± 7
331 and 160 ± 30 for the wild-type and mutant templates, respectively. Thus adding the
332 blocker led to a selective reduction in amplification, and showed that the blocker was
333 preferentially hybridised onto the wild-type strand than onto the mutant. The selected
334 concentration was 70 nm (stoichiometric ratio of 1:7 compared to the upstream primer)

335 because the biggest differences were observed at this concentration. The experiments
 336 also confirmed that the chain terminator, dideoxycytidine included in the 3'-end blocker,
 337 avoided its undesired extension by polymerase action.

338 These results were confirmed from the kinetics measurements in vials (Fig. 4). When the
 339 blocking agent was absent, a similar behaviour was observed for the wild-type and
 340 mutant solutions. Positive signals were observed after 5-10 min, and the maximum
 341 difference was achieved after 40 min of amplification. The addition of the oligonucleotide
 342 blocker preferentially inhibited the primer extension on the wild-type strands (a 40 %
 343 reduction) compared to the mutant variants (a 7% reduction).



344 **Fig. 4** Blocked RPA of *KRAS* hotspot: (a) Variation of the free energy associated with
 345 the formation of DNA duplexes (blocker-template) at 37°C. (b) Real-time RPA
 346 amplification in the solution format using DNA extracts from the wild-type (◇), mutant (○)
 347 and negative control (×) samples in the presence of blocking agent at 0 nM (continuous
 348 line) and 70 nM (discontinuous line).
 349

350

351 The versatility of method was examined, performing the enrichment of the mutant
 352 variants in three hotspots. The method was applied for the allele discrimination of *KRAS*
 353 (codon 12), *PIK3CA* (exon 9) and *PIK3CA* (exon 20). The reported data (gel
 354 electrophoresis, real-time fluorescence and solid-phase hybridization) confirmed that
 355 blocked RPA is a reliable enrichment method, because wild-type DNA amplification was
 356 minimized while mutant DNA would be promoted to be amplified (Fig. SI.4 and 5). The
 357 products from blocked RPA were effectively isolated using magnetic-core particles

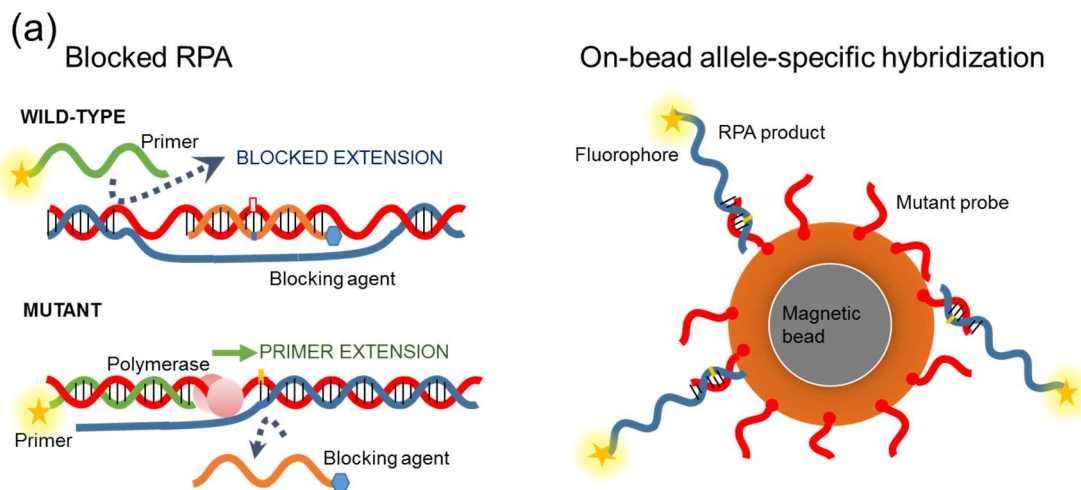
358 coated with specific probes. A selective detection was achieved (Fig. SI.6), because the
359 mutant variants provided a fluorescent bead-line with a higher signal-to-noise ratio than
360 the wild-type variant (t-test, p-value <0.05).

361 The detection capability was quantified by mixing products from the mutant and wild-type
362 genomic DNA incubated with both types of magnetic beads. To better evaluate cross-
363 reactivity, a double labelling experiment was performed. The labelling fluorophores of
364 dUTPs were 5-FAM and Cy5 for the wild-type and mutant RPA mixtures, respectively.
365 Significant fluorescent responses were obtained only in the assay when the bead was
366 conjugated to the complementary allele specific probe (Fig. 5). A relationship between
367 the responses and mutation percentage was clearly established (Fig. SI.7), and
368 demonstrated that it was possible to detect a small amount of mutant strands even in the
369 presence of large amounts of the wild-type gene.

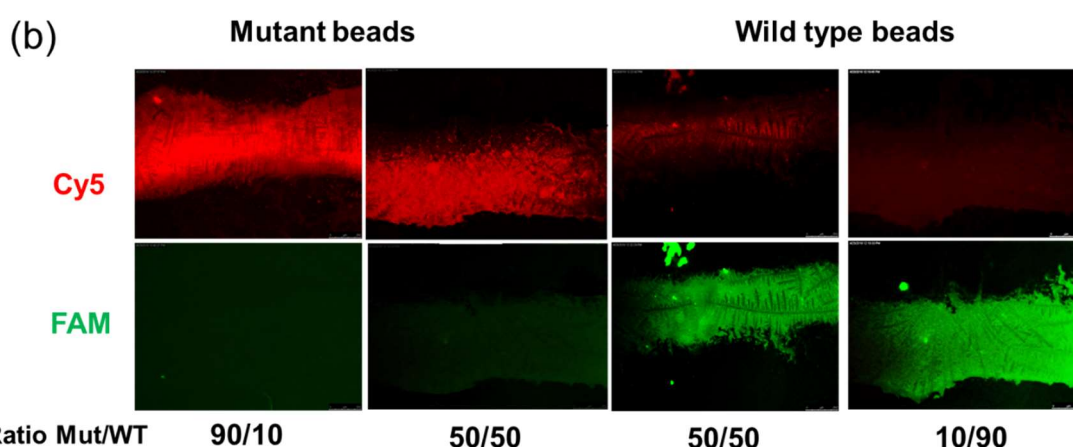
370

371 **3.5 Bead-based identification of the mutant variants**

372 The discrimination among several variants that only differ in a single nucleotide requires
373 a selective recognition and isolation. Thus the ability of selectively identifying each
374 specific mutation for a particular hotspot was investigated (*KRAS* targets: wild-type,
375 p.G12C, p.G12S, p.G12R). Blocked RPA products were aliquoted to different reactors
376 of the microfluidic chip that contained specific probe-conjugated particles. So, the
377 discriminating elements were spatially separated, but integrated into a single chip
378 (parallel assay). Under the selected conditions, each variant provided a high response
379 in the bead-line of the corresponding probe, whereas the responses associated with the
380 other probes were significantly low (t-test, p<0.005). The comparison made with the
381 heterogeneous assay confirmed the correct formation of a perfect-match hybrid between
382 the RPA product and one specific probe (Fig. 6a). Therefore, these results demonstrated
383 a selective capture, an effective concentration and, consequently, an unequivocal
384 identification (Fig. 6b).



385



386

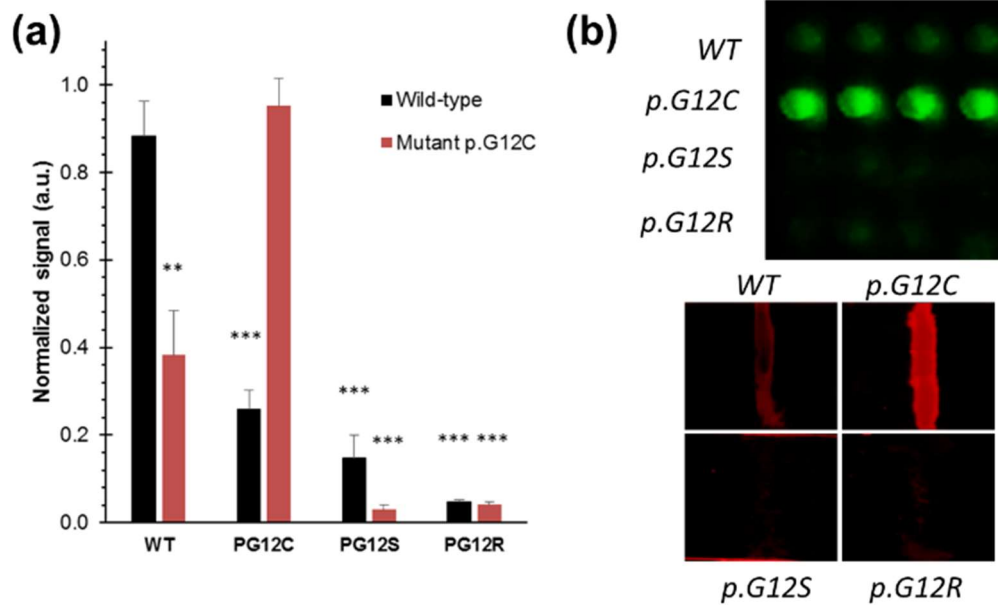
387 *Fig. 5. Mutation discrimination based on the blocked isothermal amplification and the*
 388 *allele-specific capture and concentration to the probe-conjugated magnetic particles. (a)*
 389 *Reaction schemes. (b) Fluorescence images for Cy5 and FAM channels obtained by a*
 390 *three-variable experimental design: KRAS gene p.G12C mutant/wild-type ratio (M/WT),*
 391 *labelling method (Cy5-dUTPs: mutant RPA and FAM-dUTPs: wild-type RPA) and probe-*
 392 *conjugated bead nature. Magnification factor: 10 \times . Genomic DNA: 1,333 copies.*

393

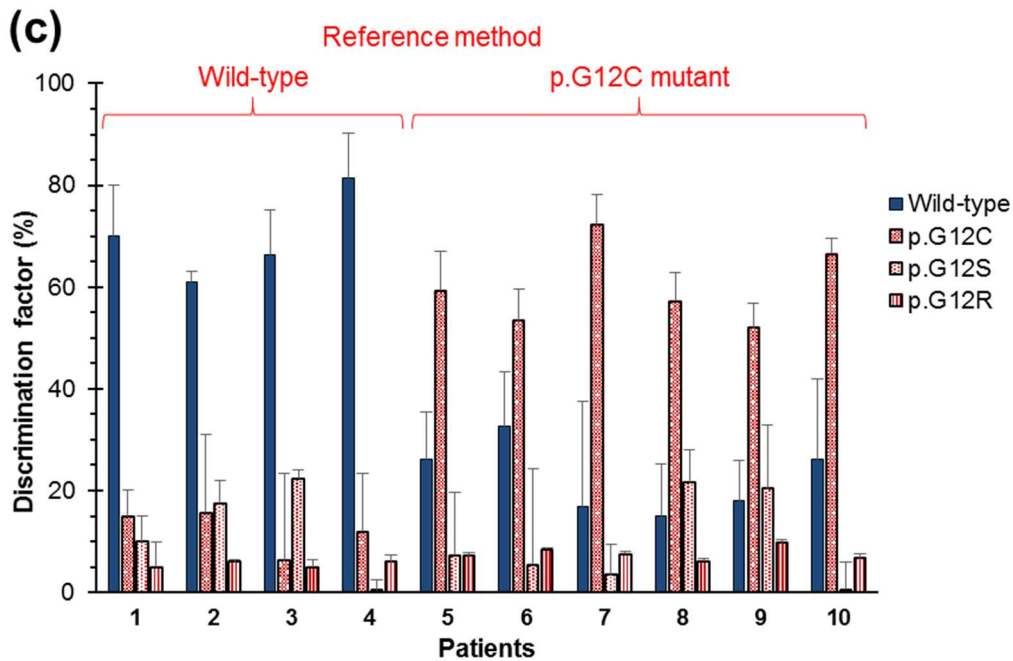
394 In a blind-assay, the developed method was applied to analyse the samples from the
 395 tumour biopsies (genomic DNA from formalin-fixed paraffin-embedded tissues). On-chip
 396 assay was parallelised for mutation detection and identification in a simple assembly
 397 (Fig. SI.8). Compared to the results obtained using the cell cultures, the inter-assay
 398 reproducibility for the tissue samples was about 2-folds worse (relative standard
 399 deviation: 20-25%) and non-specific responses were higher (30 %). Nevertheless, the
 400 population assignment was achieved by calculating of a discrimination factor based on

401 the relative responses for all the probe-conjugated beads (Fig. 6c). Four samples were
402 classified as wild-type and six samples as p.G12C mutant. These genetic variant
403 assignments agreed with the results reported by the reference method (next-generation
404 sequencing). Therefore, the hybridisation of the RPA products from complex biological
405 samples onto probe-conjugated microbeads confined within a microfluidic channel was
406 satisfactorily demonstrated.

407 Several advantages have been identified compared to similar approaches for
408 determining the mutational status of clinically relevant hotspots [6,23–25]. First, the
409 amplification at a low constant temperature (37 °C, 60 min) allowed the analysis time
410 and material resources to be reduced. Second, magnetic-induced formats are most
411 useful for developing miniaturised sensors with enhanced assay sensitivity and
412 exceptional selectivity (e.g. low-amount of DNA template, high concentration factor for
413 detection, exhaustive washing). Third, there are several compatible detection principles
414 for the cost-effective measurement of biosensing responses by enabling point-of-care
415 genetic analyses [26-27]. The developed system is aimed to fulfil the ASSURED
416 requirements described by the World Health Organization: Affordable, Sensitive,
417 Specific, User-friendly, Rapid & robust, Equipment-free, and Delivered.



418



419

420 Fig. 6. a) Normalised signal obtained for the probe-conjugated beads for a wild-type
 421 sample and a mutant sample (p.G12C). **: p-value < 0.005, ***: p-value < 0.0005. b)
 422 Image obtained for a mutant sample (p.G12C). Top: Planar chip format. Bottom: Bead
 423 format. c) Analysis of patient samples. Discrimination factor for each genetic variant was
 424 calculated from the bead-line responses. Samples were grouped based on next-
 425 generation-sequencing results.

426

427 **Conclusions**

428 In the last few decades, major progresses has been made in the DNA-based tests by
429 applying probe-coated magnetic particles in microfluidic chips. One important pending
430 challenge is to improve analytical performances for widespread exploitation, such as
431 sensitivity, selectivity, portability and fast-response. Our research addresses the problem
432 by integrating an isothermal amplification technique, which fulfils the demanded
433 requirements with excellent capabilities. The assay is performed at constant
434 temperature, with fewer needs for auxiliary instruments and by keeping the reaction
435 yields of the conventional PCR-based approach or other isothermal techniques.

436 While similar published techniques have been applied to detect large regions (tens of
437 nucleotides) or variants in synthetic templates, collected evidence has endorsed that the
438 approach here developed is able to recognise low-abundant variants of single-nucleotide
439 mutations in DNA from tumour tissues.

440 As our results have been generated using a simple prototype, more efforts are required
441 to achieve a fully-integrated device. Nevertheless, the study has demonstrated its
442 efficiency, reliability and sensitivity, as well as it has provided insights into the
443 development of innovative fast cost-effective DNA diagnostic platforms to support the
444 clinical treatment.

445

446 **Acknowledgements**

447 The authors acknowledge the financial support received from EU FEDER, the Spanish
448 Ministry of Economy and Competitiveness (MINECO project CTQ2016-75749-R and
449 Technical Support Personnel PTA- 2016).

450 **References**

- 451 [1] L.E. MacConaill, Existing and emerging technologies for tumor genomic profiling,
452 J. Clin. Oncol. 31 (2013) 1815–1824. doi:10.1200/JCO.2012.46.5948.
- 453 [2] O.Y.F. Henry, C.K. O’Sullivan, Rapid DNA hybridization in microfluidics, TrAC -
454 Trends Anal. Chem. 33 (2012) 9–22. doi:10.1016/j.trac.2011.09.014.
- 455 [3] J.P. Lafleur, A. Jönsson, S. Senkbeil, J.P. Kutter, Recent advances in lab-on-a-
456 chip for biosensing applications, Biosens. Bioelectron. 76 (2016) 213–233.
457 doi:10.1016/j.bios.2015.08.003.
- 458 [4] T. Jamshaid, E.T.T. Neto, M.M. Eissa, N. Zine, M.H. Kunita, A.E. El-Salhi, A.
459 Elaissari, Magnetic particles: From preparation to lab-on-a-chip, biosensors,
460 microsystems and microfluidics applications, TrAC - Trends Anal. Chem. 79
461 (2016) 344–362. doi:10.1016/j.trac.2015.10.022.
- 462 [5] S. Rödiger, C. Liebsch, C. Schmidt, W. Lehmann, U. Resch-Genger, U. Schedler,
463 P. Schierack, Nucleic acid detection based on the use of microbeads: A review,
464 Microchim. Acta. 181 (2014) 1151–1168. doi:10.1007/s00604-014-1243-4.
- 465 [6] T. Tangchaikeeree, D. Polpanich, A. Elaissari, K. Jangpatarapongsa, Magnetic
466 particles for in vitro molecular diagnosis: From sample preparation to integration
467 into microsystems, Colloids Surfaces B Biointerfaces. 158 (2017) 1–8.
468 doi:10.1016/j.colsurfb.2017.06.024.
- 469 [7] A. Van Reenen, A.M. De Jong, J.M.J. Den Toonder, M.W.J. Prins, Integrated lab-
470 on-chip biosensing systems based on magnetic particle actuation-a
471 comprehensive review, Lab Chip. 14 (2014) 1966–1986. doi:10.1039/c3lc51454d.
- 472 [8] S. Wang, Y. Sun, W. Gan, Y. Liu, G. Xiang, D. Wang, L. Wang, J. Cheng, P. Liu,
473 An automated microfluidic system for single-stranded DNA preparation and
474 magnetic bead-based microarray analysis, Biomicrofluidics. 9 (2015) 1–17.
475 doi:10.1063/1.4914024.
- 476 [9] V.F. Cardoso, A. Francesko, C. Ribeiro, M. Bañobre-López, P. Martins, S.
477 Lanceros-Mendez, Advances in Magnetic Nanoparticles for Biomedical
478 Applications, Adv. Healthc. Mater. 7 (2017) 1700845.
479 doi:10.1002/adhm.201700845.
- 480 [10] Y. Zhao, F. Chen, Q. Li, L. Wang, C. Fan, Isothermal Amplification of Nucleic
481 Acids, Chem. Rev. 115 (2015) 12491–12545. doi:10.1021/acs.chemrev.5b00428.

- 482 [11] C.H. Wang, K.Y. Lien, J.J. Wu, G. Bin Lee, A magnetic bead-based assay for the
483 rapid detection of methicillin- resistant *Staphylococcus aureus* by using a
484 microfluidic system with integrated loop-mediated isothermal amplification, *Lab*
485 *Chip*. 11 (2011) 1521–1531. doi:10.1039/c0lc00430h.
- 486 [12] M. Kühnemund, D. Witters, M. Nilsson, J. Lammertyn, Circle-to-circle amplification
487 on a digital microfluidic chip for amplified single molecule detection, *Lab Chip*. 14
488 (2014) 2983–2992. doi:10.1039/c4lc00348a.
- 489 [13] C. Lin, Y. Zhang, X. Zhou, B. Yao, Q. Fang, Naked-eye detection of nucleic acids
490 through rolling circle amplification and magnetic particle mediated aggregation,
491 *Biosens. Bioelectron.* 47 (2013) 515–519. doi:10.1016/j.bios.2013.03.056.
- 492 [14] I.M. Lobato, C.K. O'Sullivan, Recombinase polymerase amplification: Basics,
493 applications and recent advances, *TrAC - Trends Anal. Chem.* 98 (2018) 19–35.
494 doi:10.1016/j.trac.2017.10.015.
- 495 [15] S. Santiago-Felipe, L.A. Tortajada-Genaro, R. Puchades, Á. Maquieira, Parallel
496 solid-phase isothermal amplification and detection of multiple DNA targets in
497 microliter-sized wells of a digital versatile disc, *Microchim. Acta.* 183 (2016) 1195–
498 1202. doi:10.1007/s00604-016-1745-3.
- 499 [16] N. Dey, C. Williams, B. Leyland-Jones, P. De, Mutation matters in precision
500 medicine: A future to believe in, *Cancer Treat. Rev.* 55 (2017) 136–149.
501 doi:10.1016/J.CTRV.2017.03.002.
- 502 [17] H.S. Sloane, K.A. Kelly, J.P. Landers, Rapid KRAS Mutation Detection via
503 Hybridization-Induced Aggregation of Microbeads, *Anal. Chem.* 87 (2015) 10275–
504 10282. doi:10.1021/acs.analchem.5b01876.
- 505 [18] Y.M. Chang, S.T. Ding, E.C. Lin, L.A. Wang, Y.W. Lu, A microfluidic chip for rapid
506 single nucleotide polymorphism (SNP) genotyping using primer extension on
507 microbeads, *Sensors Actuators, B Chem.* 246 (2017) 215–224.
508 doi:10.1016/j.snb.2017.01.160.
- 509 [19] A.I. Phipps, D.D. Buchanan, K.W. Makar, A.K. Win, J.A. Baron, N.M. Lindor, J.D.
510 Potter, P.A. Newcomb, KRAS-mutation status in relation to colorectal cancer
511 survival: The joint impact of correlated tumour markers, *Br. J. Cancer.* 108 (2013)
512 1757–1764. doi:10.1038/bjc.2013.118.
- 513 [20] S. Martorell, S. Palanca, Á. Maquieira, L.A. Tortajada-Genaro, Blocked

- 514 recombinase polymerase amplification for mutation analysis of PIK3CA gene,
515 *Anal. Biochem.* 544 (2018) 49–56. doi:10.1016/j.ab.2017.12.013.
- 516 [21] A. Halperin, A. Buhot, E.B. Zhulina, Hybridization isotherms of DNA microarrays
517 and the quantification of mutation studies, *Clin. Chem.* 50 (2004) 2254–2262.
518 doi:10.1373/clinchem.2004.037226.
- 519 [22] Y. Gao, L.K. Wolf, R.M. Georgiadis, Secondary structure effects on DNA
520 hybridization kinetics: A solution versus surface comparison, *Nucleic Acids Res.*
521 34 (2006) 3370–3377. doi:10.1093/nar/gkl422.
- 522 [23] W. Shen, Y. Tian, T. Ran, Z. Gao, Genotyping and quantification techniques for
523 single-nucleotide polymorphisms, *TrAC - Trends Anal. Chem.* 69 (2015) 1–13.
524 doi:10.1016/j.trac.2015.03.008.
- 525 [24] E.S. Yamanaka, L.A. Tortajada-Genaro, N. Pastor, Á. Maquieira, Polymorphism
526 genotyping based on loop-mediated isothermal amplification and smartphone
527 detection, *Biosens. Bioelectron.* 109 (2018) 177–183.
528 doi:10.1016/j.bios.2018.03.008.
- 529 [25] I. Hernández-Neuta, I. Pereiro, A. Ahlford, D. Ferraro, Q. Zhang, J.L. Viovy, S.
530 Descroix, M. Nilsson, Microfluidic magnetic fluidized bed for DNA analysis in
531 continuous flow mode, *Biosens. Bioelectron.* 102 (2018) 531–539.
532 doi:10.1016/j.bios.2017.11.064.
- 533 [26] E.S. Yamanaka, L.A. Tortajada-Genaro, A. Maquieira, Low-cost genotyping method
534 based on allele-specific recombinase polymerase amplification and colorimetric
535 microarray detection. *Microchimica Acta*, 184 (2017) 1453-1462.
- 536 [27] A. Lázaro, E.S. Yamanaka, A. Maquieira, L.A. Tortajada-Genaro, Allele-specific
537 ligation and recombinase polymerase amplification for the detection of single
538 nucleotide polymorphisms. *Sensors Actuators, B Chem.* 298 (2019).126877.